RSC Advances

ROYAL SOCIETY OF CHEMISTRY

www.rsc.org/advances

Cite this: DOI: 10.1039/c0xx00000x

www.rsc.org/xxxxxx

COMMUNICATION

Ultra-stable glass microcraters for on-chip patch clamping

Eric Stava,*[a,b] Hyun Cheol Shin,[c] Minrui Yu,[b] Abhishek Bhat,[b] Pedro Resto,[d,e] Arjun Seshadri,[b] Justin C. Williams[c,d] and Robert H. Blick[a,b,c]

Received (in XXX, XXX) Xth XXXXXXXXX 20XX, Accepted Xth XXXXXXXXX 20XX

DOI: 10.1039/b000000x

We report on a single-step fabrication procedure of borosilicate glass micropores surrounded by a smooth microcrater. By inserting a thin air-gap between a borosilicate glass substrate and a reflective layer, we achieve dual-sided laser ablation of the device. The resultant crater provides a smoother, curved surface onto which cells settle during planar patch clamping. Gigaohm seals, which are more easily achievable on these devices as compared to conventional micropores, are achieved by patch clamping human embryonic kidney (HEK 293) cells. Further, the microcraters show enhanced mechanical stability of the planar patch clamped cells during perfusion. We integrate polydimethylsiloxane microfluidic devices with the microcraters and use passive pumping to perfuse the cells. We find that passive pumping increases the pressure within the device by 1.85 Pa. However, due to the enhanced stability of the microcrater, fluidic shearing reduces the seal resistance by only 6.8 MΩ on average, which is less than one percent of the gigaohm seal resistance.

1. Introduction

Planar patch clamping is an electrophysiological technique that allows high-throughput, on-chip electrical recordings of ion channels.[1] It is an improvement over the traditional, pipette-based patch clamping method,[2] as the glass micropipette is replaced by a micron-sized pore in a planar substrate.[3] Since multiple pores can be fabricated on a single substrate, this on-chip technique is highly parallelizable.[4-7] Planar patch clamp devices have been successful tools in drug discovery,[8-11] and show promise for low-noise ion channel screenings,[1,12] mechanosensitive studies,[13] and high-speed microfluidic perfusion.[14-18]

Planar patch clamp devices were initially fabricated in silicon substrates.[19-21] Subsequently, borosilicate glass[1] and polymetric materials[4,5] were used. Although recent experimental evidence favors the use of single-crystal quartz,[22] commercially-available techniques currently utilize borosilicate glass,[9] owing to its dielectric properties and ease of fabrication. Borosilicate glass micropores are typically fabricated by ultraviolet (UV) laser ablation.[23,24] While inexpensive and fast, this process has the unfortunate side-effect of producing molten glass debris around the rim of the micropore. The enhanced surface roughness reduces adhesion between the cell and substrate, reducing the seal resistance and increasing system noise.

In this communication, we report on an improved micropore fabrication technique. By placing a thin spacer layer between a pair of borosilicate glass substrates, we find that laser ablation of the top substrate occurs both directly from above and reflectively from below (see Fig. 1). This dual-sided laser ablation process polishes the lower side of the top substrate while drilling the micropore from above. The resultant micropore lies in a smooth, crater-like structure. This crater allows for a more natural, curved adhesion between the planar patch clamped cell and the substrate, greatly enhancing our ability to form gigaohm seals during planar patch clamping.

2. Experimental

2.1. Microcrater processing

Microcraters were fabricated by focusing a UV laser beam on the top face of a 100 μm thick borosilicate glass substrate (Carolina Biological Supply Company, Burlington, NC, USA) suspended by a thin (on the order of 100 nm) spacer over a second, glass substrate. The 193 nm ArF excimer laser (LPX-210i, Lambda Physik; optics by JP Sercel Associates, Manchester, NH, USA) was pulsed first at 50 Hz, then at 100 Hz, to ensure smooth pore formation. Software supplied by the manufacturer was used to control laser beam attenuation, repetition frequency, and number of pulses. Images in Figure 2 were made with a LEO 1530 scanning electron microscope (used both with and without tilt) following deposition of 5 nm gold onto the substrate.

2.2. Planar patch clamping

Micro-processed borosilicate glass chips were glued to plastic caps, fixed to a Port-a-Patch system (Nanion Technologies GmbH, Munich, Germany), and connected to a patch clamp amplifier (HEKA EPC 10 Single, HEKA Electronik GmbH, Lambrecht, Germany). Prior to experimentation, the glass chips were cleaned by immersion in a heated piranha bath (3:1 ratio of H_2SO_4:(30%)H_2O_2) and subsequently sonicated in deionized water. During experimentation, HEK 293 cells were immersed in a bath of 150 mM KCl, 0.2 mM $MgCl_2$, 0.2 mM ADP, 1 mM EGTA, and 10 mM HEPES[25] atop the micro-processed glass chip and negative pressure was applied to the system. In the voltage-clamp mode, large increases in resistance (gigaohm seals) revealed adhesion of a cell to the microcrater.

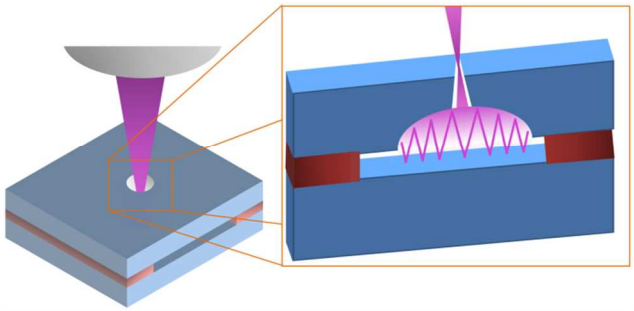

Fig. 1 A UV laser is focused on the top face of a borosilicate glass substrate and ablates the material. Ablation of the material thins the substrate, allowing for transmission of some of the laser beam through the device substrate and below, to a reflective substrate. Repeated reflections within the air-gap allow for dual-sided ablation of the bottom face of the top substrate. These reflections smooth the pore while simultaneously forming a micro-crater around it.

2.3. Microfluidics

Microfluidic devices were fabricated using traditional soft-lithography techniques.[26] Polydimethylsiloxane (PDMS) was poured over a patterned silicon wafer and allowed to cure. The PDMS microfluidic channels have dimensions of 280 µm in height, 2 mm in width, and 1 cm in length. Inlet and outlet ports (1 mm and 2 mm radii, respectively) were made using biopsy-punches (Ted Pella, Inc., Redding, CA, USA). Cells were inserted into the microfluidic device through the inlet via passive pumping. The PDMS devices were reversibly bonded to the piranha-cleaned borosilicate glass. Passive pumping was ensured prior to experimentation by flowing the electrophysiological solution through the microfluidic device.

A 5 µL drop placed at the inlet, which collapses in approximately 0.17 seconds, gives an average flow rate of 2.3 mL/min (calculated from equations given in ref. 27; see Supplemental Information). It is important to note that flow during passive pumping is a function of how a drop collapses into the inlet of the device. This type of flow is pulse-like in nature. As calculated by theory, the highest flow rate within the channel under these conditions is 2.9 mL/min, but this flow lasts for less than 15 ms. The average and maximum shear stresses associated with these flow rates are 1.44 Pa and 1.85 Pa, respectively.

2.4. Cell culturing

We used HEK 293 cells (CRL 1573, American Type Culture Collection) for planar patch clamping, cultured at 37 °C with 5% CO_2. The cells were cultured in a medium consisting of minimum essential medium (MEM) with L-glutamine and Earle's salts (Invitrogen, Carlsbad, CA, USA), supplemented with 0.1 mM MEM amino acids solution, 1 mM sodium pyruvate, 1% penicillin/streptomycin, and 10% fetal bovine serum (Harlan Laboratories, Indianapolis, IN, USA).

3. Results and discussion

3.1. Microcrater fabrication

Figure 1 outlines the fabrication process. We focus a UV laser beam on the top surface of the device substrate and ablate the material. Material ablation begins with a low repetition rate, high energy beam to thin the device, and is immediately followed with a high repetition rate, low energy beam to finalize pore formation. As the device is processed, the laser energy that is not absorbed by the device substrate transmits through it, to the air-gap, where it is reflected by the lower substrate. Proper tuning of the air-gap thickness allows for repeated reflections within the air-gap cavity. We find that these repeated reflections induce backside ablation of the device substrate, which smoothes the substrate in the immediate vicinity of the micropore while simultaneously forming a concave, crater-like structure.

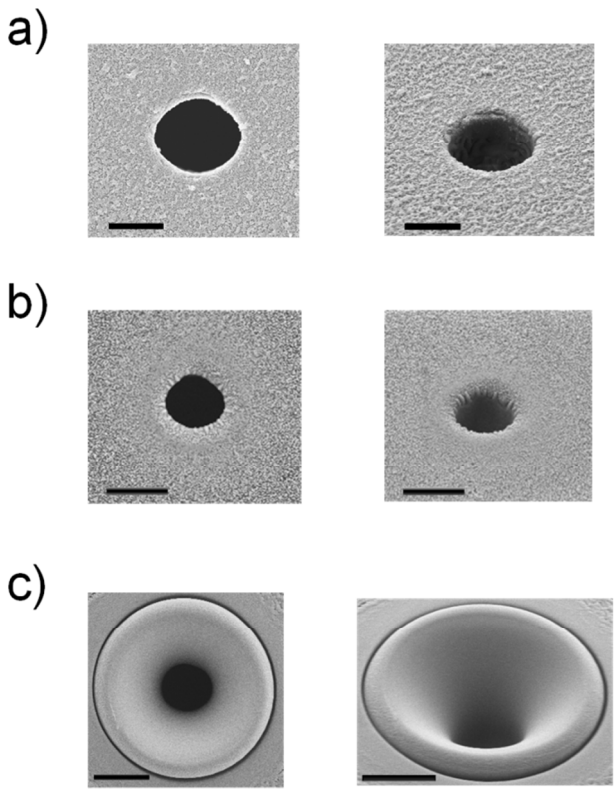

Fig. 2 (a) Normal and tilt views of a micropore formed in borosilicate glass without a lower, reflective substrate. (b) A micropore formed with the same laser recipe as that in (a), but with a large (order of microns) air-gap below the substrate. (c) A microcrater formed with the same recipes used in (a) and (b), but with a thin (order of 100 nm) air-gap between the device substrate and the reflective substrate. All scale bars are 2 µm.

Figure 2 shows the results from laser-ablation of borosilicate glass without a reflective substrate (Fig. 2a), with a reflective substrate but without proper tuning of the air-gap thickness (Fig. 2b), and with both a reflective substrate and proper air-gap tuning (Fig. 2c). The laser parameters for all three cases are the same. In the latter case (Fig. 2c), the average pore diameter is 2.95 µm and the average microcrater diameter is 10.36 µm (n = 11). The pore diameter is therefore similar to those used commercially for planar patch clamping, while the crater diameter is commensurate with cell dimensions. Since the final pore diameter in the latter case is similar to those in the former cases, it would be feasible to reduce the pore diameter to the UV wavelength by tuning the laser parameters,[23] though this would affect the microcrater as well. Figure 2c also displays the smooth surface of the microcrater in the direct vicinity of the micropore, which enhances cell adhesion during planar patch clamping. Further,

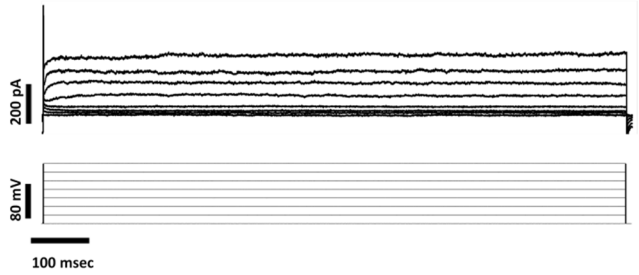

Fig. 3 Voltage-clamp response of HEK 293 cells planar patch clamped to our microcraters (seal resistance is ~ 1.6 GΩ).

we find that improper air-gap thicknesses do not form this polished, microcrater structure. We find that spacing on the order of the wavelength of the laser light is ideal for repeated reflections between the two substrates. However, a three-fold increase in air-gap thickness does not produce a microcrater when the same laser ablation parameters are used (for a comparison of these two cases, see Fig. 2b,c).

3.2 HEK 293 patch clamp

We found that patch clamped gigaohm seals form much more readily with our microcraters than with commercially-available planar patch clamp micropores. Figure 3 shows the voltage clamp response from a planar patch clamped HEK 293 cell over a microcrater. Following suspension of HEK 293 cells in the *cis* compartment, the application of negative pressure guides the cell to the microcrater, where a gigaohm seal forms in a matter of seconds (a seal resistance of 1.6 GΩ is given for the result in Fig. 3). The whole-cell, voltage-clamp mode was achieved by "zapping" the cell with bursts of voltage and pressure, with minimal loss in seal resistance. Subsequent application of voltage steps result in the opening of voltage-gated ion channels, which correspond to the current traces in Fig. 3. Comparable results were obtained by either leaving the *cis* chamber open to ambient or confining it with a microfluidic device.

3.3 Microfluidic perfusion

A further advantage of using microcraters for planar patch clamping is the improved mechanical stability achieved by the cell. This is of critical importance when perfusing the cell, or when studying its mechanosensitive properties. We demonstrate this improved mechanical stability by perfusing planar patch clamped cells enclosed in a microfluidic device with an electrophysiological solution (see Fig. 4). We use microfluidic devices with inlet and outlet ports open to ambient pressure, since this allows for inexpensive and straight-forward perfusion of the cell via surface-tension passive pumping,[28] though it should be noted that rapid fluid exchanges using inertia enhanced passive pumping are also possible in this configuration.[29] Surface-tension passive pumping moves liquid from a higher-pressure, smaller drop at the inlet port to a lower-pressure, larger drop at the outlet port.[28] In this way, microfluidic perfusion is achieved by simply adding subsequent, small droplets to the inlet.

By passive pumping the same electrolyte solution over a microcrater-planar patch clamped cell (Fig. 4c) we mechanically perturb the cell, resulting in an average change in seal resistance of 6.8 MΩ (n = 7), although individual trials can be quite low (Fig. 4c). This change in seal resistance constitutes less than one

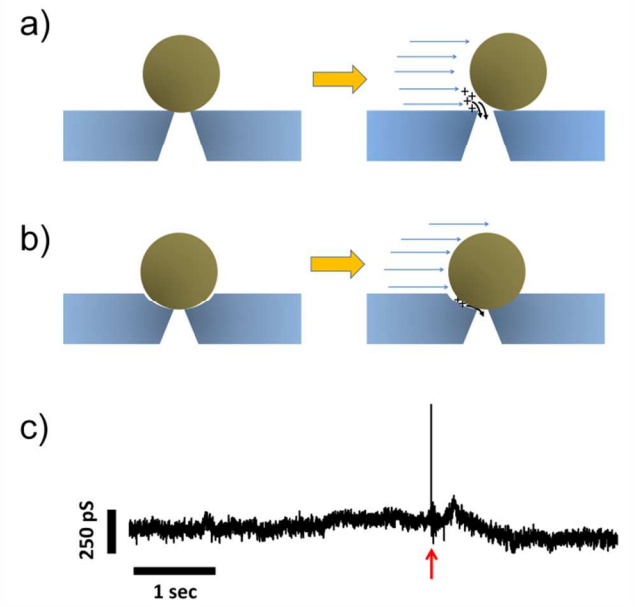

Fig. 4 Action of fluidic force on a planar patch clamped cell during perfusion. (a) Without a microcrater, the planar patch clamped cell is less likely to withstand shear, fluidic forces. (b) The microcrater mechanically enhances the stability of the cell during perfusion. (c) Voltage-clamp response of a planar patch clamped cell undergoing passive pumping of the electrophysiological solution. A red arrow indicates the insertion of the passive pumping droplet. The seal resistance in this particular example is reduced by 0.64 MΩ.

percent of a giga-seal and, therefore, guarantees stable, electrical results during microfluidic perfusion. Although the relative flow rate used is not particularly high, the exchange rates can be very rapid using this technique.[29] Therefore, the cell stability shown here is a necessary step in the further integration of planar patch clamp techniques with high-speed fluidic exchange.

Conclusions

In summary, we have shown that dual-sided laser ablation of borosilicate glass is a novel micropore formation method for planar patch clamping, and that it is superior to those methods used by commercial vendors. We have shown that our microcrater substrates easily integrate with microfluidic devices, and that microfluidic perfusion has negligible impact on the seal resistance. Since our procedure utilizes UV wavelengths, the laser parameters can be tuned to produce remarkably smaller pores.[23,30] Furthermore, tuning of the air-gap spacing and reflective material could be used to enhance control over the crater-micropore structure, thereby tuning the system to the particular cell type under investigation.

Acknowledgements

The authors would like to acknowledge funding from DARPA (MOLDICE-program, Grant #49620-03-1-03837) and the Wisconsin Institute for Discovery Pilot Program.

Notes and references

[a] *Institut für Angewandte Physik, Universität Hamburg, Jungiusstr. 11, 20355 Hamburg, Germany. Fax: +49-40-428-38-6332; Tel: +49-40-42838-2910; E-mail: estava@physnet.uni-hamburg.de*
[b] *Department of Electrical and Computer Engineering, University of Wisconsin-Madison, 1415 Engineering Dr., Madison, WI 53706, USA*
[c] *Materials Science Program, University of Wisconsin-Madison, 1415 Engineering Dr., Madison, WI 53706, USA*
[d] *Department of Biomedical Engineering, University of Wisconsin-Madison, 1415 Engineering Dr., Madison, WI 53706, USA*
[e] *Mechanical Engineering Department, University of Puerto Rico at Mayagüez, 259 Boulevard Alfonso Valdes, Mayagüez, Puerto Rico 00680*

1 N. Fertig, R. H. Blick and J. C. Behrends, *Biophys J,* 2002, **82**, 3056-3062.
2 B. Sakmann and E. Neher, *Single Channel Recordings,* New York: Pflenum, 1995.
3 N. Fertig, Ch. Meyer, R. H. Blick, Ch. Trautmann and J. C. Behrends, *Phys Rev E,* 2001, **64**, 040901.
4 K. G. Klemic, J. F. Klemic, M. A. Reed and F. J. Sigworth, *Biosens Bioelectron,* 2002, **17**, 597-604.
5 L. Kiss, P. B. Bennett, V. N. Uebele, K. S. Koblan, S. A. Kane, B. Neagle and K. Schroeder, *Assay Drug Dev Technol,* 2003, **1**, 127-135.
6 B. Matthews and J. W. Judy, *J MEMS,* 2006, **15,** 214-222.
7 A. Brüggeman, S. Stoelzl, M. George, J. C. Behrends and N. Fertig, *Small*, 2006, **2**, 840-846.
8 C. Wood, C. Williams and G. J. Waldron, *Drug Discov Today,* 2004, **9**, 434-441.
9 J. Dunlop, M. Bowlby, R. Peri, D. Vasilyev and R. Arias, *Nature Rev Drug Discovery,* 2008, **7**, 358-368.
10 C. J. Milligan, J. Li, P. Sukumar, Y. Majeed, M. L. Dallas, A. English, P. Emery, K. E. Porter, A. M. Smith, I. McFadzean, D. Beccano-Kelly, Y. Bahnasi, A. Cheong, J. Naylor, F. Zeng, X. Liu, N. Gamper, L.-H. Jiang, H. A. Pearson, C. Peers, B. Robertson and D. J. Beech, *Nat Protoc,* 2009, **4,** 244-255.
11 C.-Y. Chen, T.-Y. Tu, D.-S. Jong and A. M. Wo, *Biotechnol Bioeng,* 2011, **108**, 1395-1403.
12 M. Mayer, J. K. Kriebel, M. T. Tosteson and G. M. Whitesides, *Biophys J*, 2003, **85**, 2684-2695.
13 E. Stava, M. Yu, H. C. Shin, H. Shin, J. Rodriguez and R. H. Blick, *Lab Chip,* 2012, **12,** 80-87.
14 C. Ionescu-Zanetti, R. M. Shaw, J. Seo, Y.-N. Jan, L. Y. Jan and L. P. Lee, *Proc Nat Acad Sci USA,* 2005, **102,** 9112-9117.
15 X. Li, K. G. Klemic, M. A. Reed and F. J. Sigworth, *Nano Letters,* 2006, **6**, 815-819.
16 T. Sordel, S. Garnier-Raveaud, F. Sauter, C. Pudda, F. Marcel, M. De Waard, C. Arnoult, M. Vivaudou, F. Chatelain and N. Picollet-D'hahan, *J Biotechnol,* 2006, **125**, 142-154.
17 A. Y. Lau, P. J. Hung, A. R. Wu and L. P. Lee, *Lab Chip,* 2006, **6,** 1510-1515.
18 N. Bao, J. Wang and C. Lu, *Anal Bioanal Chem*, 2008, **391**, 933-942.
19 C. Schmidt, M. Mayer and H. Vogel, *Angew Chem,* 2000, **112,** 3267-3270.
20 N. Fertig, A. Tilke, R. H. Blick, J. P. Kotthaus, J. C. Behrends and G. ten Bruggencate, *App Phys Lett*, 2000, **77**, 1218-1220.
21 R. Pantoja, D. Sigg, R. Blunck, F. Bezanilla and J. R. Heath, *Biophys J,* 2001, **81**, 2389-2394.
22 E. Stava, M. Yu, H. C. Shin and R. H. Blick, *IEEE Trans Nanobiosci,* 2010, **9**, 307-309.
23 M. Yu, H.-S. Kim and R. H. Blick, *Opt Express,* 2009, **17,** 10044.
24 C.-Y. Chen, T.-Y. Tu, C.-H. Chen, D.-S. Jong and A. M. Wo, *Lab Chip*, 2009, **9**, 2370-2380.
25 G. Zhu, Y. Zhang, H. Xu and C. Jiang, *J Neurosci Methods,* 1998, **81**, 73-83.
26 D. C. Duffy, J. C. McDonald, O. J. A. Schueller and G. M. Whitesides, *Anal Chem,* 1998, **70**, 4974-4984.
27 E. Berthier and D. J. Beebe, *Lab Chip*, 2007, **7**, 1475-1478.
28 G. M. Walker and D. J. Beebe, *Lab Chip,* 2002, **2**, 131-134.
29 P. J. Resto, E. Berthier, D. J. Beebe and J. C. Williams, *Lab Chip,* 2012, **12**, 2221-2228.
30 E. Stava, M. Yu, H. C. Shin, H. Shin, D. J. Kreft and R. H. Blick, *Lab Chip*, 2013, **13**, 156-160.

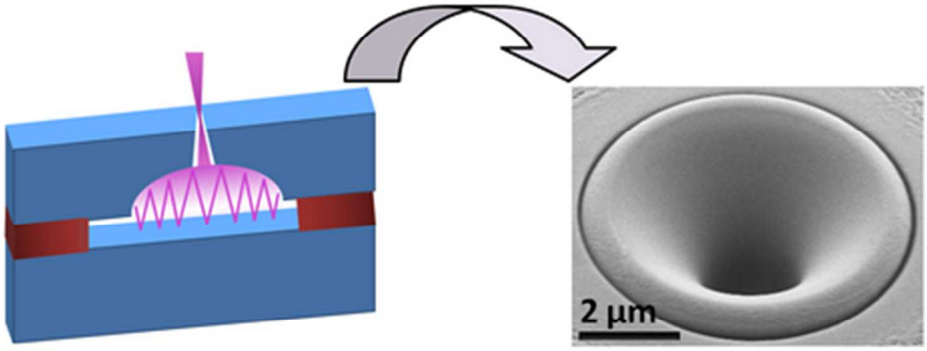

Dual-sided laser ablation is used to form glass microcraters commensurate with the size of a cell. These microcraters allow for ultra-stable, low noise recordings of planar patch-clamped cells.
39x19mm (300 x 300 DPI)